crystallization communications

Crystallization and X-ray diffraction analysis of the DNA-remodelling protein DnaD from *Bacillus subtilis*

Sabine Schneider,[a] **Maria J. V. M. Carneiro,**[b] **Charikleia Ioannou,**[b] **Panos Soultanas**[b]* **and Max Paoli**[a]*

[a]School of Pharmacy and Centre for Biomolecular Sciences, University of Nottingham, England, and [b]School of Chemistry and Centre for Biomolecular Sciences, University of Nottingham, England

Correspondence e-mail: panos.soultanas@nottingham.ac.uk, max.paoli@nottingham.ac.uk

The DnaD protein is an essential component of the chromosome-replication machinery of the Gram-positive bacterium *Bacillus subtilis* and is part of the primosomal cascade that ultimately loads the replicative ring helicase DnaC onto DNA. Moreover, DnaD is a global regulator of DNA architecture, as it forms higher order nucleoprotein structures in order to open supercoiled DNA. Here, the crystallization and preliminary X-ray diffraction analysis of the two domains of DnaD from *B. subtilis* are reported. Crystals of the N-terminal domain are trigonal, with either $P3_121$ or $P3_221$ space-group symmetry, and diffracted X-rays to 2.0 Å resolution; crystals of the C-terminal domain are hexagonal, with space group $P6_1$ or $P6_5$, and diffracted X-rays to 2.9 Å resolution in-house. Determination of the structure of the DnaD domains will provide insight into how remodelling of the nucleoid is associated with priming of replication in the model Gram-positive organism *B. subtilis*.

1. Introduction

Initiation of bacterial DNA replication involves the remodelling of a replication origin (*ori*C) through the action of the initiator protein DnaA and this is followed by a series of molecular events, known as the primosomal cascade, that ultimately result in the loading of two replicative ring helicases, one onto each strand of the duplex DNA. DNA primases are then recruited by helicases, thus signalling the switch from initiation to elongation; as a result, two replication forks start to migrate in opposite directions on the leading and the lagging strands (Fang *et al.*, 1999; Marszalek & Kaguni, 1994). Progression to the elongation stage does not guarantee completion of DNA replication, as the replication forks could accidentally be arrested anywhere along the DNA. In *Escherichia coli*, an active replication fork at arrested sites is reconstituted by the primosomal pathways, which include the PriA, PriB, PriC and DnaT proteins (Marians, 2000; Ng & Marians, 1996), while priming at the *ori*C is mediated by DnaA. Both DnaA and PriA have homologues in Gram-positive bacteria such as *Bacillus subtilis* and other Gram-positive bacteria. In addition, another essential primosomal cascade involving the DnaD, DnaB and DnaI proteins is found in these Gram-positive bacteria. While DnaI is believed to be the Gram-positive functional homologue of the *E. coli* helicase-loader, both the DnaD and DnaB primosomal proteins have no homologues in Gram-negative bacteria and their exact functions are still being explored. They are essential for viability and are required for DnaA- and PriA-mediated initiation of DNA replication (Bruand *et al.*, 2001; Moriya *et al.*, 1999). At present, the molecular events of the priming mechanism are unclear, but data from various experiments indicate that DnaD interacts with DnaA, PriA and DnaB (Ishigo-Oka *et al.*, 2001; Marsin *et al.*, 2001), while DnaI interacts with the DnaC helicase (Imai *et al.*, 2000; Noirot-Gros *et al.*, 2002; Soultanas, 2002). DnaD is believed to act early in the cascade, setting the stage for the helicase recruitment by a helicase-loader constituted of both DnaB and DnaI (Velten *et al.*, 2003).
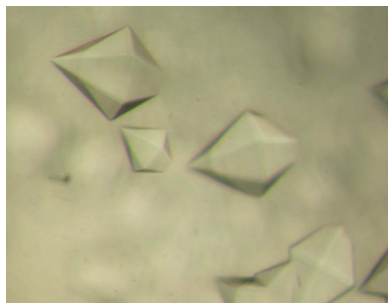
Table 1
Statistics for the processing and merging of the diffraction data.

Values in parentheses are for the highest resolution shell.

	DnaD N-domain	DnaD C-domain
Space group	$P3_121/P3_221$	$P6_1/P6_5$
Unit-cell parameters (Å)		
a (Å)	78.6	57.8
b (Å)	78.6	57.8
c (Å)	124.5	50.8
α (°)	90.0	90.0
β (°)	90.0	90.0
γ (°)	120.0	120.0
Wavelength (Å)	1.5418	1.5418
Resolution range (Å)	28.0–2.0 (2.1–2.0)	15.0–2.9 (3.1–2.9)
No. of observations	177843 (25869)	22589 (2331)
No. of unique reflections	30662 (4429)	2161 (294)
Multiplicity	5.8 (5.8)	10.5 (7.9)
Completeness (%)	99.8 (100.0)	98.3 (92.8)
R_{sym}† (%)	4.8 (37.6)	9.5 (37.2)
Mean $I/\sigma(I)$	24.4 (4.0)	20.4 (4.6)
Solvent content (%)	62.9 or 25.8	39.7
Matthews coefficient (Å^3 Da^{-1})	3.3 or 1.6	2.0
Molecules per ASU	2 or 4	2

† $R_{sym} = \sum_h \sum_i |I_{h,i} - \langle I_h \rangle| / \sum_h \sum_i |I_{h,i}|$, where the outer summation is over all unique reflections with multiple observations and the inner summation is over all observations of each reflection.

Recently, it was discovered that DnaD and DnaB have opposing global DNA-remodelling activities. DnaD interacts with linear DNA, forming a nucleoprotein structure with a round DnaD scaffold in the middle holding the DNA in an open circle around the periphery, whereas DnaB compacts laterally supercoiled and linear DNA (Turner *et al.*, 2004; Zhang *et al.*, 2005). Moreover, DnaD converts all the writhe of a supercoiled plasmid into twist (Zhang *et al.*, 2005). The biological significance of these activities is not clear at present, but a functional model has been proposed with DnaD and DnaB being the link between global or local DNA remodelling and the initiation of DNA replication (Turner *et al.*, 2004; Zhang *et al.*, 2005). The function of DnaD is thought to be similar to the HU and H-NS proteins in *E. coli*. DnaD consists of two domains: oligomerization activity has been attributed to the N-terminal domain (N-domain), while the C-terminal domain (C-domain) binds DNA and has an additional DNA-induced oligomerization activity (Carneiro *et al.*, 2006). The untagged full-length protein is 232 residues in length and has a molecular weight of 27 490 Da; the N-domain includes residues 1–128 and has a molecular weight of 16 056 Da (including the His tag) and the C-domain includes residues 129–232 and has a molecular weight of 13 730 Da (including the His tag). The sequence of DnaD has no significant similarity to any protein in the Protein Data Bank and therefore appears to have a unique signature. Revealing the structure–function relationships of the DNA-remodelling roles of DnaD is an aim of high biological significance as it will lead to a better understanding of how remodelling of the bacterial nucleoid is associated with replication priming in the Gram-positive model organism *B. subtilis*. Here, we report the crystallization and preliminary X-ray diffraction analysis of the two domains of DnaD.

2. Methods

2.1. Cloning, expression and purification

The N-domain and C-domain of DnaD from *B. subtilis* were cloned and purified by nickel-affinity chromatography as previously described (Carneiro *et al.*, 2006). Briefly, *E. coli* BL21 (DE3) cells were grown at 310 K and 200 rev min^{-1} until an OD$_{600}$ of 0.6 was reached. Protein expression was then induced by adding IPTG to a

final concentration of 1 m*M* and cultures were grown for a further 7–8 h. The cells were lysed by sonication and the lysate was clarified by centrifugation. Purification was carried out in 50 m*M* phosphate buffer pH 7.5, 100 m*M* NaCl using a HiTrap Ni^{2+}-chelating column (Amersham Biosciences) and gel filtration in 50 m*M* Tris pH 7.5, 100 m*M* NaCl, 1 m*M* DTT (Superdex 75, Amersham Biosciences). Protein samples in the gel-filtration buffer mentioned above were flash-frozen in liquid nitrogen for storage at 193 K after the addition of glycerol to a final concentration of 10%(*v*/*v*). Protein samples were thawed prior to crystallization and concentrated to 15–20 mg ml^{-1} using centrifugal membrane devices (Vivaspin) without exchanging the buffer.

2.2. Crystallization

Initially, high-throughput crystallization screening was carried out using the Hydra II micro-dispensing system (Robbins Hydra, Matrix Technologies Ltd, Wilmslow, Engand) with the sitting-drop vapour-diffusion method in 96-well microtitre plates (Greiner). Conditions from six crystallization screens, Classics, PEGs, AmSO$_4$, Cations, MPDs and OptiSalts (Nextal Biotechnology/Qiagen), were tested with a protein concentration of 15–20 mg ml^{-1}, a drop size of 0.6 + 0.6 µl and a reservoir volume of 100 µl. Crystallization plates were left undisturbed in a Sanyo MIR-253 incubator at 293 K. Small single crystals (0.07 × 0.09 × 0.03 mm) of the N-domain were obtained in 0.1 *M* sodium acetate pH 4.6, 3.2 *M* sodium chloride. Crystals of the N-domain were improved by manual screening in sitting-drop vapour-diffusion experiments using 24-well Cryschem plates
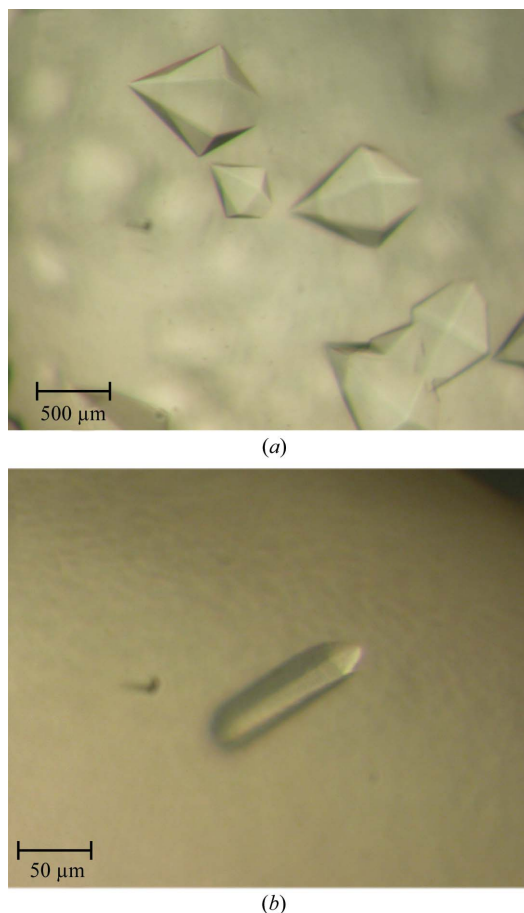

(a)

(b)

Figure 1
Crystals of (*a*) the N-domain and (*b*) the C-domain of DnaD.

(Hampton Research) with drop sizes of either 4 + 4 µl or 8 + 8 µl and a protein concentration of 20 mg ml^{-1}.

2.3. Data collection and analysis

Prior to flash-freezing, crystals of the DnaD N-domain were transferred to cryoprotected artificial mother liquor containing 0.1 M sodium acetate pH 4.6, 3.3 M sodium chloride and 0.85 M sodium malonate (Holyoak *et al.*, 2003). C-domain crystals obtained in 2.2 M ammonium sulfate and 0.2 M sodium malonate were transferred to a cryoprotected artificial mother liquor consisting of 2.4 M ammonium sulfate and 1 M sodium malonate prior to flash-freezing.

Data collections from both N-domain and C-domain crystals were carried out in-house using a Rigaku MicroMax 007 rotating-anode generator with a rotating copper anode (operating at 40 kV and 20 mA) equipped with VariMax HF optics (Osmic, Rigaku), an R-AXIS IV++ image-plate detector and an X-stream 2000 cryo-cooling vapour jet. Diffraction data were processed using the programs *MOSFLM* v.6.2.4 (Leslie, 1992) and *SCALA* (Evans, 1997) as included in the *CCP*4 suite (Collaborative Computational Project, Number 4, 1994).

3. Results

We have established conditions for the growth of diffraction-quality crystals of both the N-domain and C-domain of the *B.subtilis* DNA-remodelling protein DnaD. The best results for the DnaD N-domain were obtained using 25–100 mM sodium acetate pH 4.6 and 2.7–3.3 M sodium chloride and crystals typically appeared after 4–6 d and grew to dimensions of 0.8 × 0.6 × 0.6 mm. (Fig. 1a). Approximately two weeks after they first appeared, crystals of the N-domain started to
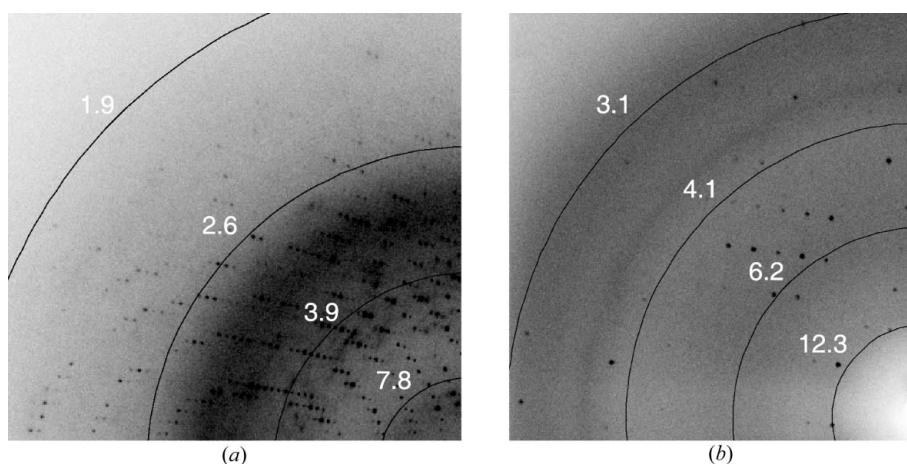

Figure 2
Diffraction pattern obtained from crystals of (*a*) the N-domain and (*b*) the C-domain of DnaD recorded using a home source.
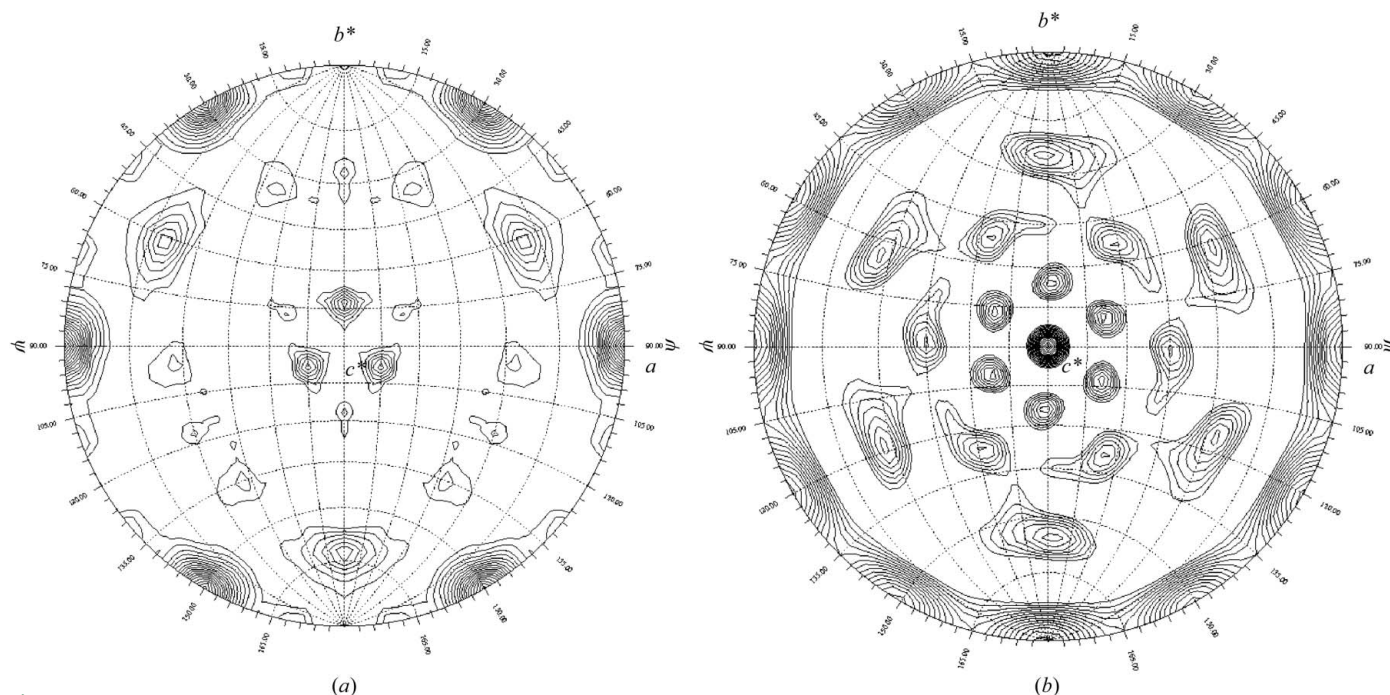

Figure 3
Self-rotation function of (*a*) the N-domain and (*b*) the C-domain calculated using the program *GLRF* (Tong & Rossmann, 1997). In this analysis, data between 9 and 4 Å resolution were used; the figure shows the section for $\kappa = 180°$ with a 20 Å integration radius.

lose their quality and degrade. Crystals of the C-domain (Fig. 1b) grew in various conditions containing ammonium sulfate, either by itself (2.2 M) or in combination with one of the following salts (all at 0.2 M): ammonium fluoride, potassium acetate, potassium fluoride, sodium malonate, sodium sulfate decahydrate, sodium formate or sodium fluoride. Despite these crystallization conditions differing slightly, the C-domain crystals had similar shape and size: they were very small, $0.02 \times 0.02 \times 0.1$ mm, and required over four weeks to grow. As already performed for the N-domain, the optimization of growth conditions for the C-domain crystals is in progress; the preliminary X-ray analysis reported below was carried out with C-domain crystals mounted straight from the 96-well plates.

The crystals are of sufficiently high quality to allow X-ray structure determination. The diffraction of the N-domain crystals extended to 2.0 Å resolution (Fig. 2a) and 100° of data were collected with 0.5° oscillations and an exposure time of 7 min. The crystal of the C-domain diffracted to 2.9 Å and a data set was collected consisting of 180 frames with 1° oscillations and 12 min exposure times (Fig. 2b). The lattice symmetry of the N-domain crystals belongs to the enantiomorphic trigonal space groups $P3_121$ or $P3_221$, whereas the C-domain crystallizes with hexagonal symmetry and belongs to the enantiomorphic space groups $P6_1$ or $P6_5$. While our analysis was assisted by the program POINTLESS (Collaborative Computational Project, Number 4, 1994), the diffraction data were also processed in alternative space groups, but the resulting high R_{sym} values led us to rule out other possible symmetries. The statistics of the crystal unit-cell parameters and data processing are shown in Table 1. Solvent-content and Matthews coefficient calculations on both domains suggest that two to four molecules pack in the asymmetric unit of the N-domain, while one or two molecules are believed to make up the asymmetric unit of the C-domain crystals. A self-rotation function analysis on the data at $\kappa = 180°$ was carried out using the program GLRF (Tong & Rossmann, 1997). This analysis indicates the presence of at least one twofold noncrystallographic symmetry axis for both the N-domain and C-domain lattices (Fig. 3). Thus, the N-domain asymmetric unit is expected to consist of either a dimer or a tetramer, while based on solvent-content calculations the C-domain can only contain a dimer in the asymmetric unit. Determination of the structure of the N-domain using the SeMet MAD method should be possible given the presence of five methionine residues in its 128-amino-acid sequence. For the C-domain, which has no methionine residues, this method cannot be used unless mutations of leucine and/or isoleucine residues to methionine are carried out. Elucidation of the structure of DnaD and/or of its domains will provide insights into the function of this unique protein essential for B. subtilis and lead to a better understanding of its role in nucleoid-remodelling associated with priming of DNA replication.

References

Bruand, C., Farache, M., McGovern, S., Ehrlich, S. D. & Polard, P. (2001). *Mol. Microbiol.* **42**, 245–255.

Carneiro, M. J., Zhang, W., Ioannou, C., Scott, D. J., Allen, S., Roberts, C. J. & Soultanas, P. (2006). *Mol. Microbiol.* **60**, 917–924.

Collaborative Computational Project, Number 4 (1994). *Acta Cryst.* D**50**, 760–763.

Evans, P. (1997). *Jnt CCP4/ESF–EACMB Newsl. Protein Crystallogr.* **33**, 22–24.

Fang, L., Davey, M. J. & O'Donnell, M. (1999). *Mol. Cell,* **4**, 541–553.

Holyoak, T., Fenn, T. D., Wilson, M. A., Moulin, A. G. & Ringe, D. (2003). *Acta Cryst.* D**59**, 2356–2358.

Imai, Y., Ogasawara, N., Ishigo-Oka, D., Kadoya, R., Daito, T. & Moriya, S. (2000). *Mol. Microbiol.* **36**, 1037–1048.

Ishigo-Oka, D., Ogasawara, N. & Moriya, S. (2001). *J. Bacteriol.* **183**, 2148–2150.

Leslie, A. G. W. (1992). *Jnt CCP4/ESF–EACMB Newsl. Protein Crystallogr.* **26**.

Marians, K. J. (2000). *Trends Biochem. Sci.* **25**, 185–189.

Marsin, S., McGovern, S., Ehrlich, S. D., Bruand, C. & Polard, P. (2001). *J. Biol. Chem.* **276**, 45818–45825.

Marszalek, J. & Kaguni, J. M. (1994). *J. Biol. Chem.* **269**, 4883–4890.

Moriya, S., Imai, Y., Hassan, A. K. & Ogasawara, N. (1999). *Plasmid,* **41**, 17–29.

Ng, J. Y. & Marians, K. J. (1996). *J. Biol. Chem.* **271**, 15642–15648.

Noirot-Gros, M. F., Dervyn, E., Wu, L. J., Mervelet, P., Errington, J., Ehrlich, S. D. & Noirot, P. (2002). *Proc. Natl Acad. Sci. USA,* **99**, 8342–8347.

Soultanas, P. (2002). *Nucleic Acids Res.* **30**, 966–974.

Tong, L. & Rossmann, M. G. (1997). *Methods Enzymol.* **276**, 594–611.

Turner, I. J., Scott, D. J., Allen, S., Roberts, C. J. & Soultanas, P. (2004). *FEBS Lett.* **577**, 460–464.

Velten, M., McGovern, S., Marsin, S., Ehrlich, S. D., Noirot, P. & Polard, P. (2003). *Mol. Cell,* **11**, 1009–1020.

Zhang, W., Carneiro, M. J., Turner, I. J., Allen, S., Roberts, C. J. & Soultanas, P. (2005). *J. Mol. Biol.* **351**, 66–75.